Supporting Information

Exploring the Mechanism of Isomerisation and Water-Migration in the Water-Complexes of Amino-acid L-Proline: Electrostatic Potential and Vibrational Analysis

Gurpreet Kaur and Vikas*

Quantum Chemistry Group, Department of Chemistry & Centre of Advanced Studies in Chemistry, Panjab University, Chandigarh- 160014 INDIA.

*Corresponding author (Email: qlabspu@pu.ac.in, qlabspu@yahoo.com)

Table of contents

Figure S1. Isomerisation channels of conformers of L-proline obtained through GRRM. The geometries (with bond length in Å) are optimized at HF/6-31G level of theory and the values refers to *ZPE* corrected energy (in a.u.).

Figure S2. Same as Figure S1 but for Neutral/zwitterion isomerisation pathways of lowest lying conformers of L-proline.

Figure S3. Same as Figure S1, but for isomerisation of L-proline single-water complexes.

Figure S4. Transition states governing the automerisation routes between L-proline-water complexes at the BHandHLYP/6-311++G(d,p) level of the theory. The values refer to *ZPE* and *BSSE* corrected relative energies (in kcal/mol) with respect to Complex 4b obtained at the CCSD(T)/6-311++G(d,p)//BHandHLYP/6-311++G(d,p) level of the theory.

Table S1. Relative energies (in kcal/mol) of four lowest-lying conformers (Ps) and transition states (TSs), depicted in Figure 1, with respect to P1 at the *ZPE* corrected DFT/BHandHLYP/6-311++G(d,p) and CCSD(T)/6-311++G(d,p)//DFT/BHandHLYP/6-311++G(d,p) levels of the theory. The values compared in parentheses are from Ref. [11] computed at the B3LYP/6-311++G(d,p) level of the theory. The transition state represented as TS P*n*/P*m* connects the *n*th isomer of L-proline with *m*th isomer.

Table S2. Relative energies(in kcal/mol) of *L*-Proline–water complexes and interconnecting transition states with respect to Complex 4b depicted in Figs. 2–4 at ZPE and BSSE corrected (1) DFT/BHandHLYP/6-311++G(d,p), and (2) CCSD(T)/6-311++G(d,p)//BHandHLYP/6-311++G(d,p) levels of the theory. The stabilization energy(in kcal/mol) of these complexes are represented in bold, and the values compared in parenthesis are from Ref. 11 computed at the B3LYP/6-311++G(d,p) level of the theory without ZPE and BSSE corrections.

Table S3. Second order interaction energies, $E^{(2)}$ (in kcal/mol), representing the strength of H-bond formed between *L*-proline and single water molecules at BHandHLYP/6-311++G(d,p).

Table S4. Relative shifts in the scaled [Ref.47] vibrational (IR) frequency (in cm^{-1}), along with the corresponding intensity (in km/mol) depicted in parenthesis, and Raman activity (in Å/a.m.u.), for relevant vibrational modes in various conformers of L-Proline, with respect to those in the lowest lying conformer P1, at DFT/BHandHLYP/6-311++G(d,p) level of the theory.

Table S5. Relative shifts in the scaled [Ref.47] vibrational (IR) frequency (in cm^{-1}), along with the corresponding intensity (in km/mol) depicted in parenthesis, and Raman activity (in Å/a.m.u.), for relevant vibrational modes in various complexes of L-proline with single-water molecule, with respect to lowest-lying Complex 2c among class I & II complexes, at DFT/BHandHLYP/6-311++G(d,p) level of the theory.

Table S6. Relative shifts in the scaled [Ref.47] vibrational (IR) frequency (in cm^{-1}), along with the corresponding intensity (in km/mol) depicted in parenthesis, and Raman activity (in Å/a.m.u.), for relevant vibrational modes in various complexes of *L*-proline with single water molecule with respect to lowest-lying Complex 4b at DFT/BHandHLYP/6-311++G(d,p) level of the theory.

Table S7. Comparison of experimental frequencies and intensity from Ref. [51] with that of computed at BHandHLYP/6-311++G(d,p) with frequencies scaled with correction factor of 0.9335[Ref.47] for conformers P1 and P4. Values in parenthesis were computed at B3LYP/aug-cc-pVDZ level of the theory reported in previous work[Ref. 51].

Table S8. Relative shifts in the scaled [Ref.47] vibrational (IR) frequency (in cm^{-1}), along with the corresponding intensity (in km/mol) depicted in parenthesis, and Raman activity (in Å/a.m.u.), for relevant vibrational with respect to P1, at DFT/BHandHLYP/6-311++G(d,p) level of the theory.

Table S9. Relative shifts in the scaled [Ref.47] vibrational (IR) frequency (in cm^{-1}), along with the corresponding intensity (in km/mol) depicted in parenthesis, and Raman activity (in Å/a.m.u.), for relevant vibrational with respect to P2, at DFT/BHandHLYP/6-311++G(d,p) level of the theory.

Table S10. Relative shifts in the scaled [Ref.47] vibrational (IR) frequency (in cm^{-1}), along with the corresponding intensity (in km/mol) depicted in parenthesis, and Raman activity (in Å/a.m.u.), for relevant vibrational with respect to P3, at DFT/BHandHLYP/6-311++G(d,p) level of the theory.

Table S11. Relative shifts in the scaled [Ref.47] vibrational (IR) frequency (in cm^{-1}), along with the corresponding intensity (in km/mol) depicted in parenthesis, and Raman activity (in Å/a.m.u.), for relevant vibrational with respect to P4, at DFT/BHandHLYP/6-311++G(d,p) level of the theory.

Table S12. Standard Gibbs free energy change (ΔG) in kcal/mol, at various temperatures, for the dissociation pathways at BHandHLYP/6-311++G(d,p) level of the theory depicted in supporting information Figure S1.

Input and options applied in some calculations

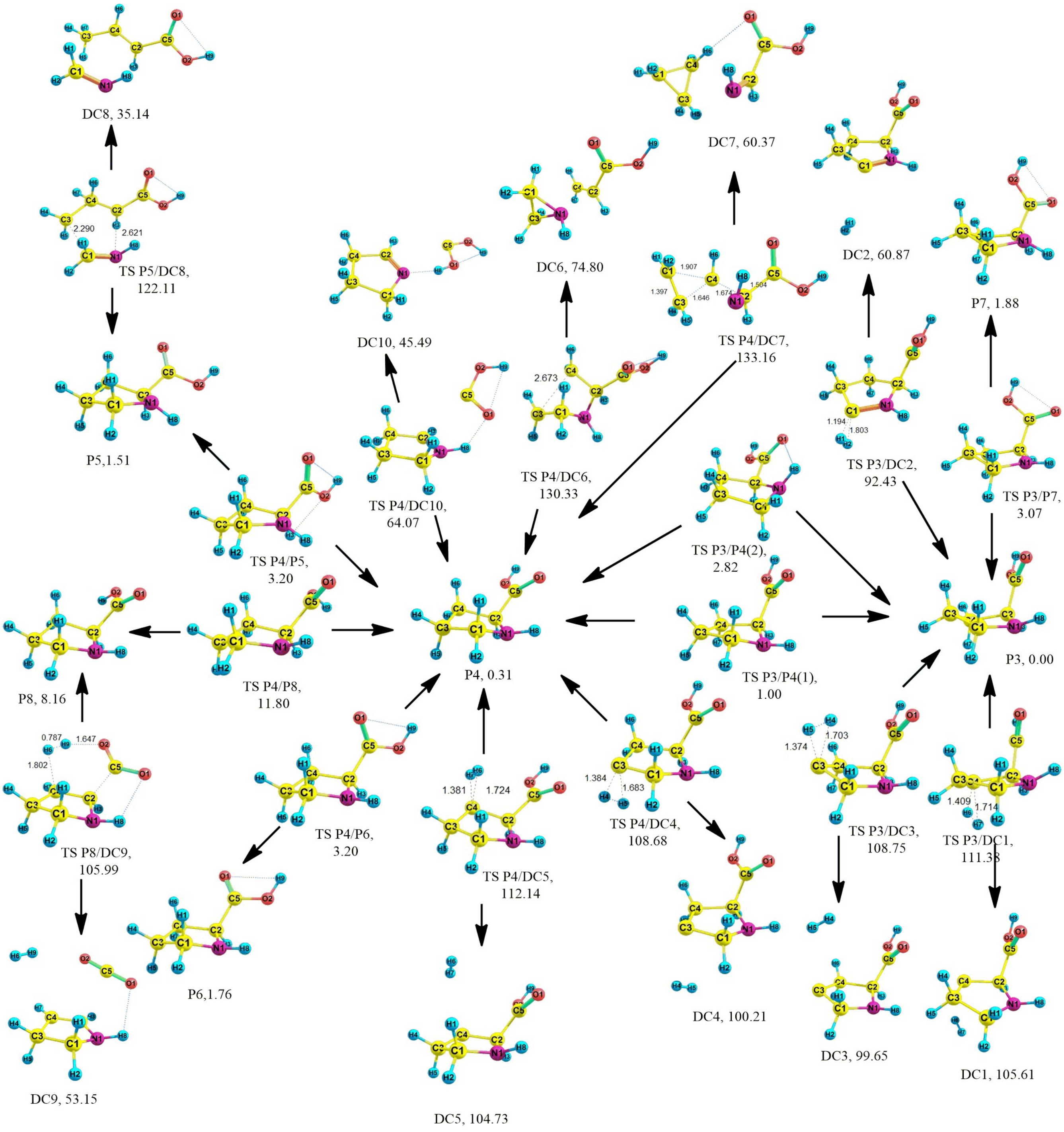

Figure S1. Isomerisation channels of conformers of L-proline obtained through GRRM. The geometries (with bond length in Å) are optimized at HF/6-31G level of theory and the values refers to *ZPE* corrected energy (in a.u.).

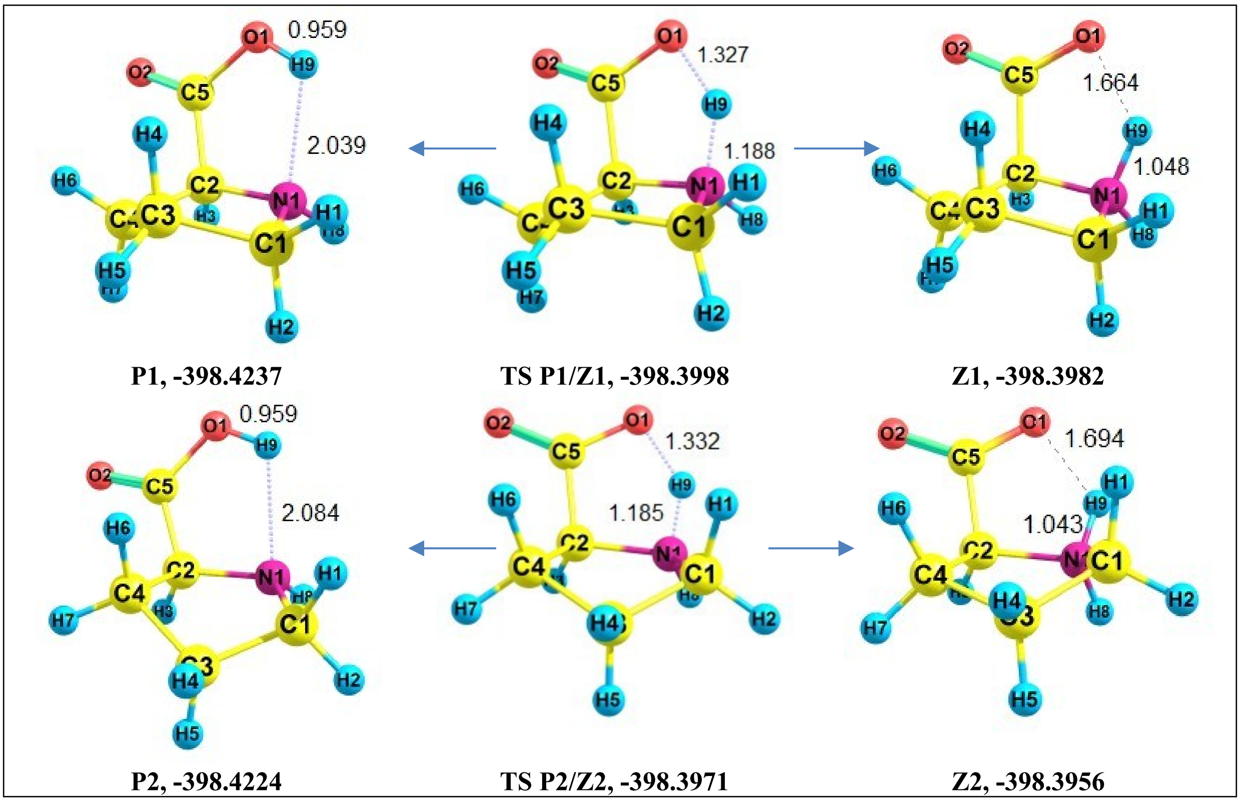

P1, -398.4237 **TS P1/Z1, -398.3998** **Z1, -398.3982**

P2, -398.4224 **TS P2/Z2, -398.3971** **Z2, -398.3956**

Figure S2. Same as Figure S1 but for Neutral/zwitterion isomerisation pathways of lowest lying conformers of L-proline.

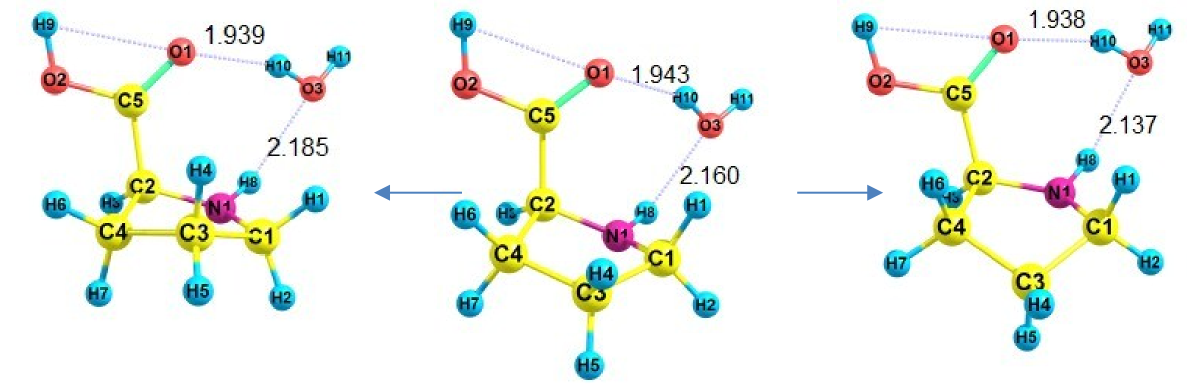

Complex 3a, -474.4081 **Complex TS 3a/4a, -474.4066** **Complex 4a, -474.4077**

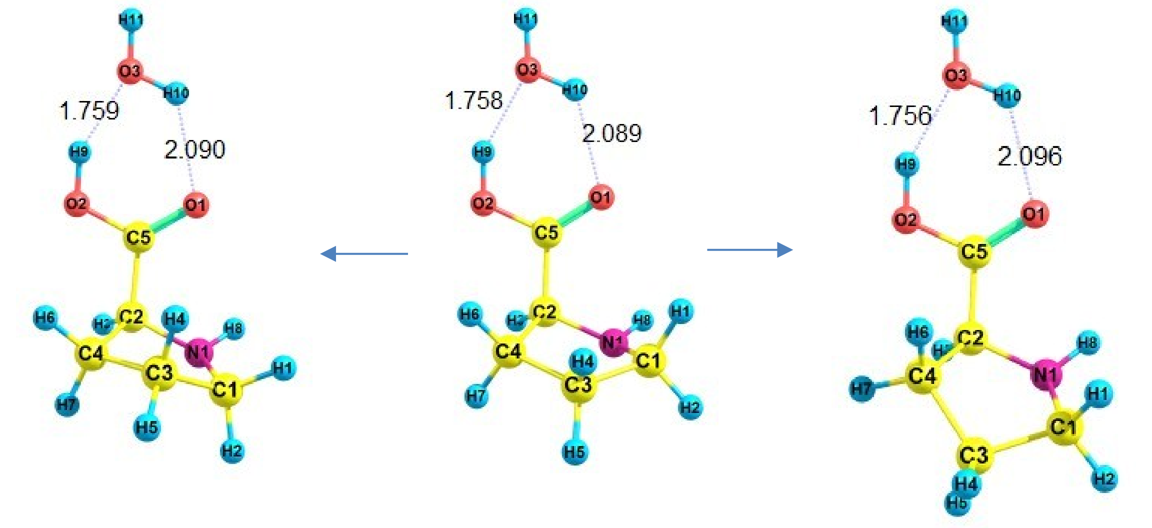

Complex 3b, -474.4003 **Complex TS 3b/4b, -474.3987** **Complex 4b -474.3995**

Figure S3. Same as Figure S1, but for isomerisation of L-proline single-water complexes.

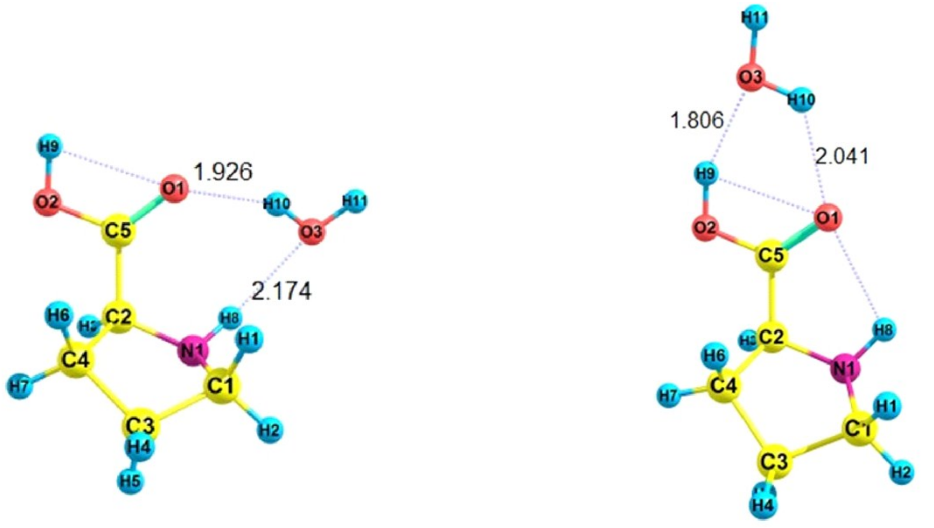

Complex TS 4a/4a
2.45

Complex TS 4b/4b
0.25

Figure S4. Transition states governing the automerisation routes between L-proline-water complexes at the BHandHLYP/6-311++G(d,p) level of the theory. The values refer to *ZPE* and *BSSE* corrected relative energies (in kcal/mol) with respect to Complex 4b obtained at the CCSD(T)/6-311++G(d,p)//BHandHLYP/6-311++G(d,p) level of the theory.

Table S1. Relative energies (in kcal/mol) of four lowest-lying conformers (Ps) and transition states (TSs), depicted in Figure 1, with respect to P1 at the *ZPE* corrected DFT/BHandHLYP/6-311++G(d,p) and CCSD(T)/6-311++G(d,p)//DFT/BHandHLYP/6-311++G(d,p) levels of the theory. The values compared in parentheses are from Ref. [11] computed at the B3LYP/6-311++G(d,p) level of the theory. The transition state represented as TS P*n*/P*m* connects the *n*th isomer of L-proline with *m*th isomer.

Spieces	ZPE	BHandHLYP/6-311++G(d,p)	CCSD(T)/6-311++G(d,p)// BHandHLYP/6-311++G(d,p)
P1	0.00	0.00(0.00)	0.00
P2	0.13	0.38(0.44)	0.50
P3	0.44	0.88(1.75)	1.51
P4	0.50	0.56(1.40)	1.38
TS P1/P2	0.13	1.69	1.69
TS P3/P4(1)	0.50	1.44	1.95
TS P3/P4(2)	0.56	1.82	2.26

Table S2. Relative energies(in kcal/mol) of L-Proline–water complexes and interconnecting transition states with respect to Complex 4b depicted in Figs. 2–4 at ZPE and BSSE corrected (1) DFT/BHandHLYP/6-311++G(d,p), and (2) CCSD(T)/6-311++G(d,p)//BHandHLYP/6-311++G(d,p) levels of the theory. The stabilization energy(in kcal/mol) of these complexes are represented in bold, and the values compared in parenthesis are from Ref. 11 computed at the B3LYP/6-311++G(d,p) level of the theory without ZPE and BSSE corrections.

Complexes	BHandHLYP/6-311++G(d,p)		BSSE(1)	ZPE	CCSD(T)/6-311++G(d,p)// BHandHLYP/6-311++G(d,p)	BSSE(2)
Complex 1a	5.90(5.13)	**11.11**	1.13	0.44	4.08	3.39
Complex 1b	2.89(2.26)	**5.96**	0.63	-0.31	0.82	1.57
Complex 1c	1.69(1.24)	**7.72**	0.50	0.06	0.25	1.95
Complex 1d	3.70(3.00)	**5.27**	0.69	-0.25	1.00	2.13
Complex 1e	3.64(2.91)	**4.64**	0.69	-0.88	1.07	1.76
Complex 2a	5.84(4.84)	**10.92**	1.44	0.56	4.71	4.08
Complex 2b	3.45(2.68)	**5.96**	0.63	-0.31	1.38	1.57
Complex 2c	1.63(3.66)	**8.16**	0.50	0.00	0.06	1.88
Complex 2d	4.33(3.33)	**5.21**	0.69	-0.31	1.32	2.20
Complex 2e	4.14(3.28)	**4.64**	0.69	-0.88	1.63	1.82
Complex 3a	3.64(4.47)	**6.78**	0.56	-0.56	2.51	2.13
Complex 3b	0.25(0.32)	**10.67**	0.88	0.00	0.06	2.70
Complex 3c	6.28(6.30)	**3.64**	0.50	-0.75	4.02	1.63
Complex 3d	2.82(2.46)	**7.66**	0.75	-0.19	1.00	2.26
Complex 3e	4.58	**8.22**	1.07	-0.25	2.70	2.95
Complex 4a	3.70(4.05)	**6.46**	0.69	-0.56	2.70	2.26
Complex 4b	0.00(0.00)	**10.60**	0.88	0.00	0.00	2.64
Complex 4c	5.33(5.76)	**3.89**	0.50	-1.00	3.64	1.57
Complex 4d	2.64(2.25)	**7.59**	0.82	-0.13	1.07	2.38
Complex Z1	12.24	**13.49**	0.75	0.50	10.92	2.64
Complex Z2	14.12	**12.24**	0.75	0.31	12.93	2.64
Complex TS1a/1b	6.09		0.82	-0.94	4.33	2.38
Complex TS1b/1c	2.82		0.44	-0.44	0.88	1.44
Complex TS1c/1d	3.77		0.75	-0.31	0.88	2.26
Complex TS1a/1d[a]	6.09		0.82	-0.94	4.27	2.38
Complex TS2b/2c[a]	3.26		0.44	-0.50	1.44	1.38
Complex TS1a/2a	6.53		1.00	0.00	5.21	3.14
Complex TS1b/2b	4.83		0.63	-0.38	2.76	1.63
Complex TS1d/2d	5.46		0.75	-0.38	2.70	2.13
Complex TS1a/Z1	18.76		1.95	-3.26	21.27	8.66
Complex TS2a/Z2	18.57		2.13	-2.95	21.65	8.97
Complex TS3a/3b	4.83		0.50	-0.88	3.39	1.57
Complex TS3b/3c	6.28		0.38	-1.13	4.46	1.13
Complex TS3d/3e[a]	46.75		1.13	-0.50	48.44	6.02
Complex TS3a/3e	5.77		0.63	-1.38	5.40	2.07
Complex TS4a/4b	4.52		0.50	-0.94	3.26	1.51
Complex TS4b/4c	5.96		0.38	-1.19	4.27	1.19
Complex TS4a/4d	67.65		1.19	-3.07	71.98	9.41
Complex TS3c/4c	6.71		0.56	-1.00	4.58	1.69
Complex TS3d/4d	4.33		1.26	-0.38	7.03	7.40
Complex TS4a/4a	3.45		0.56	-0.75	2.45	2.07
Complex TS4b/4b	0.31		0.69	-0.44	0.25	2.07

[a] TS obtained from the double ended TS search option in GRRM. Except these, all other TSs are obtained by saddle point optimization.

[b] Complex TS *n*/*m* specifies the transition state connects the *n*th complex of proline-single water molecule with *m*th complex.

Table S3. Second order interaction energies, $E^{(2)}$ (in kcal/mol), representing the strength of H-bond formed between *L-proline* and single water molecules at BHandHLYP/6-311++G(d,p).

Complex	Donor Acceptor	$E^{(2)}$	Donor Acceptor	$E^{(2)}$
	Proline H_2O		H_2O Proline	
Complex 1a	$n_{N1(1)} \rightarrow \sigma^*_{O3\text{-}H10}$	13.98	$n_{O3(1)} \rightarrow \sigma^*_{O1\text{-}H9}$	0.22
	$n_{N1(1)} \rightarrow \sigma^*_{O3\text{-}H11}$	0.14	$n_{O3(2)} \rightarrow \sigma^*_{O1\text{-}H9}$	17.69
Complex 1b	$n_{O2(1)} \rightarrow \sigma^*_{O3\text{-}H10}$	1.37		
	$n_{O2(2)} \rightarrow \sigma^*_{O3\text{-}H10}$	4.12		
Complex 1c	$n_{O2(1)} \rightarrow \sigma^*_{O3\text{-}H10}$	2.19	$n_{O3(2)} \rightarrow \sigma^*_{C2\text{-}H3}$	0.28
	$n_{O2(2)} \rightarrow \sigma^*_{O3\text{-}H10}$	6.77		
Complex 1d	$n_{O1(1)} \rightarrow \sigma^*_{O3\text{-}H11}$	0.94	$n_{O3(1)} \rightarrow \sigma^*_{C3\text{-}H4}$	0.21
	$n_{O1(2)} \rightarrow \sigma^*_{O3\text{-}H11}$	2.37	$n_{O3(2)} \rightarrow \sigma^*_{C3\text{-}H4}$	1.11
	$n_{O1(2)} \rightarrow \sigma^*_{O3\text{-}H10}$	0.08		
Complex 1e			$n_{O3(2)} \rightarrow \sigma^*_{N1\text{-}H11}$	4.54
Complex 2a	$n_{N1(1)} \rightarrow \sigma^*_{O3\text{-}H10}$	14.46	$n_{O3(1)} \rightarrow \sigma^*_{O1\text{-}H9}$	0.20
	$n_{N1(1)} \rightarrow \sigma^*_{O3\text{-}H11}$	0.12	$n_{O3(2)} \rightarrow \sigma^*_{O1\text{-}H9}$	17.60
Complex 2b	$n_{O2(1)} \rightarrow \sigma^*_{O3\text{-}H11}$	1.36		
	$n_{O2(2)} \rightarrow \sigma^*_{O3\text{-}H11}$	4.08		
Complex 2c	$n_{O2(1)} \rightarrow \sigma^*_{O3\text{-}H11}$	2.36	$n_{O3(1)} \rightarrow \sigma^*_{C4\text{-}H7}$	0.09
	$n_{O2(2)} \rightarrow \sigma^*_{O3\text{-}H11}$	7.10	$n_{O3(2)} \rightarrow \sigma^*_{C4\text{-}H7}$	0.52
Complex 2d	$n_{O1(1)} \rightarrow \sigma^*_{O3\text{-}H11}$	0.42	$n_{O3(1)} \rightarrow \sigma^*_{C1\text{-}H1}$	0.40
	$n_{O1(2)} \rightarrow \sigma^*_{O3\text{-}H11}$	2.00	$n_{O3(2)} \rightarrow \sigma^*_{C4\text{-}H8}$	0.40
	$n_{O1(2)} \rightarrow \sigma^*_{O3\text{-}H10}$	0.11		
Complex 2e			$n_{O3(2)} \rightarrow \sigma^*_{N1\text{-}H11}$	4.67
Complex 3a	$n_{O1(1)} \rightarrow \sigma^*_{H10\text{-}O3}$	3.16	$n_{O3(1)} \rightarrow \sigma^*_{C1\text{-}H1}$	0.23
	$n_{O1(2)} \rightarrow \sigma^*_{H10\text{-}O3}$	4.10	$n_{O3(2)} \rightarrow \sigma^*_{N1\text{-}H8}$	1.64
Complex 3b	$n_{O1(1)} \rightarrow \sigma^*_{H10\text{-}O3}$	0.99	$n_{O3(1)} \rightarrow \sigma^*_{O2\text{-}H9}$	0.16
	$n_{O1(2)} \rightarrow \sigma^*_{H10\text{-}O3}$	3.61	$n_{O3(2)} \rightarrow \sigma^*_{O2\text{-}H9}$	14.89
	$n_{O1(2)} \rightarrow \sigma^*_{O3\text{-}H11}$	0.11		
Complex 3c	$n_{O2(1)} \rightarrow \sigma^*_{H10\text{-}O3}$	3.01	$n_{O3(2)} \rightarrow \sigma^*_{C2\text{-}H3}$	0.22
Complex 3d	$n_{N1(1)} \rightarrow \sigma^*_{H8\text{-}O3}$	13.34	$n_{O3(2)} \rightarrow \sigma^*_{C2\text{-}H3}$	0.06
Complex 3e	$n_{N1(1)} \rightarrow \sigma^*_{H10\text{-}O3}$	9.91		
	$n_{O1(2)} \rightarrow \sigma^*_{H10\text{-}O3}$	0.09		
Complex 4a	$n_{O1(1)} \rightarrow \sigma^*_{H10\text{-}O3}$	2.64	$n_{O3(1)} \rightarrow \sigma^*_{N1\text{-}H8}$	0.09
	$n_{O1(2)} \rightarrow \sigma^*_{H10\text{-}O3}$	2.84	$n_{O3(2)} \rightarrow \sigma^*_{N1\text{-}H8}$	3.20
Complex 4b	$n_{O1(1)} \rightarrow \sigma^*_{H10\text{-}O3}$	1.04	$n_{O3(1)} \rightarrow \sigma^*_{O2\text{-}H9}$	0.16
	$n_{O1(2)} \rightarrow \sigma^*_{H10\text{-}O3}$	3.81	$n_{O3(2)} \rightarrow \sigma^*_{O2\text{-}H9}$	14.55
	$n_{O1(2)} \rightarrow \sigma^*_{O3\text{-}H11}$	0.11		
Complex 4c	$n_{O2(1)} \rightarrow \sigma^*_{O3\text{-}H11}$	3.42	$n_{O3(1)} \rightarrow \sigma^*_{C4\text{-}H7}$	0.30
			$n_{O3(2)} \rightarrow \sigma^*_{C4\text{-}H7}$	0.23
			$n_{O3(2)} \rightarrow \sigma^*_{C2\text{-}H3}$	0.07
Complex 4d	$n_{N1(1)} \rightarrow \sigma^*_{H8\text{-}O3}$	13.21		
Complex Z1	$n_{O1(1)} \rightarrow \sigma^*_{H9\text{-}O3}$	1.63	$n_{O3(1)} \rightarrow \sigma^*_{N1\text{-}H8}$	0.09
	$n_{O1(2)} \rightarrow \sigma^*_{H9\text{-}O3}$	1.98	$n_{O3(2)} \rightarrow \sigma^*_{N1\text{-}H8}$	1.24
	$n_{O1(3)} \rightarrow \sigma^*_{H9\text{-}O3}$	5.71	$n_{O3(1)} \rightarrow \sigma^*_{N1\text{-}H10}$	0.10
Complex Z2	$n_{O1(1)} \rightarrow \sigma^*_{H9\text{-}O3}$	4.29	$n_{O3(1)} \rightarrow \sigma^*_{N1\text{-}H10}$	0.20
	$n_{O1(2)} \rightarrow \sigma^*_{H9\text{-}O3}$	1.06	$n_{O3(2)} \rightarrow \sigma^*_{N1\text{-}H10}$	0.11
	$n_{O1(3)} \rightarrow \sigma^*_{H9\text{-}O3}$	7.12	$n_{O3(2)} \rightarrow \sigma^*_{C1\text{-}H1}$	1.96

where *n* denotes the donation of lone pair from lewis structure to σ^* antibond of non-lewis structure

Table S4. Relative shifts in the scaled [Ref.47] vibrational (IR) frequency (in cm^{-1}), along with the corresponding intensity (in km/mol) depicted in parenthesis, and Raman activity (in Å/a.m.u.), for relevant vibrational modes in various conformers of L-Proline, with respect to those in the lowest lying conformer P1, at DFT/BHandHLYP/6-311++G(d,p) level of the theory.

Modes Conformers	*v* (C=O) IR shift	Raman shift	*v* (C-O) IR shift	Raman shift	*v*(O-H) IR shift	Raman shift	*v*(N-H) IR shift	Raman shift
P1*	0.0 (0.0)	0.0	0.0 (0.0)	0.0	0.0 (0.0)	0.0	0.0 (0.0)	0.0
P2	1.63 (13.66)	0.43	-2.41 (46.33)	0.627	18.19 (-143.70)	29.97	0.31 (121.11)	-42.06
P3	-28.83 (-76.76)	-1.95	-263.12 (-158.65)	-1.286	249.05 (-213.17)	48.68	-18.20 (18.25)	-34.00
P4	-26.98 (-60.28)	-0.59	-261.40 (-129.39)	-1.112	248.52 (-214.94)	55.82	-12.06 (11.76)	-18.99

*The IR frequency of vibrational modes, *v*(C=O), *v*(C-O), *v*(O-H) and *v*(N-H), in P1 is 1800.44, 1382.31, 3425.64, and 3451.55 cm^{-1}, respectively, with corresponding intensity of 413.12, 364.395, 318.673, 10.139 km/mol. The Raman activity of these modes, respectively, is 11.202, 2.445, 59.432, and 72.836 Å/a.m.u..

Table 5. Relative shifts in the scaled [Ref.47] vibrational (IR) frequency (in cm^{-1}), along with the corresponding intensity (in km/mol) depicted in parenthesis, and Raman activity (in Å/a.m.u.), for relevant vibrational modes in various complexes of L-proline with single-water molecule, with respect to lowest-lying Complex 2c among class I & II complexes, at DFT/BHandHLYP/6-311++G(d,p) level of the theory.

	L-Proline								water	
Modes Complexes	*v* (C=O) IR shift	Raman shift	*v* (C-O) IR shift	Raman shift	*v*(O-H) IR shift	Raman shift	*v*(N-H) IR shift	Raman shift	*v*(O-H) IR shift	Raman shift
Complex 1a	6.11 (-160.35)	-1.75	-84.84 (-162.55)	2.50	51.87 (799.32)	-18.64	-71.54 (35.63)	59.81	-106.33 (765.65)	-63.20
Complex 1b	12.20 (-22.76)	-0.01	-9.17 (-23.95)	-0.40	-13.53 (42.79)	-0.80	3.45 (1.11)	14.29	83.09 (-63.85)	29.33
Complex 1c	-1.45 (-11.68)	-0.36	-0.99 (-85.58)	-0.91	-22.52 (21.16)	-3.08	-0.17 (0.53)	15.89	6.82 (-11.19)	3.89
Complex 1d	32.33 (-54.82)	-1.59	-10.34 (-13.21)	0.16	268.35 (-227.59)	26.08	5.11 (0.038)	18.50	-207.65 (5.09)	-51.53
Complex 1e	22.63 (-36.76)	-0.58	2.97 (24.89)	0.04	-36.97 (50.13)	0.00	-21.82 (137.50)	45.92	152.81 (-334.55)	-13.61
Complex 2a	6.54 (-62.71)	3.69	-45.28 (-122.75)	-0.52	43.02 (618.62)	-26.38	-46.77 (-1.17)	21.23	-115.19 (584.94)	-70.94
Complex 2b	13.99 (-8.24)	0.56	-9.42 (22.87)	0.17	242.33 (-27.47)	77.56	1.26 (0.37)	-1.21	-149.32 (-12.40)	-42.04
Complex 2c*	0.00 (0.00)	0.00	0.00 (0.00)	0.00	0.00 (0.00)	0.00	0.00 (0.00)	0.00	0.00 (0.00)	0.00
Complex 2d	33.57 (-40.69)	-0.70	-8.34 (25.80)	0.78	-33.62 (7.06)	-8.25	-5.05 (-2.89)	7.23	114.89 (-294.25)	-23.74
Complex 2e	24.29 (-24.60)	-0.27	0.65 (50.15)	0.98	-10.49 (33.44)	7.92	-21.81 (128.45)	24.95	152.54 (-334.35)	-16.56
Complex Z1	-43.15 (49.78)	-4.27					-603.72 (415.07)	-27.20	-74.31 (37.09)	-13.20
Complex Z2	-43.21 (107.04)	-4.15					-583.11 (428.66)	-31.56	-85.96 (116.07)	-6.65

*The scaled IR frequency of vibrational modes *v*(C=O), *v* (C-O), *v*(O-H), *v*(N-H) and v_{sym}(O-H, H_2O) in complex 2c is 1773.49, 1392.63, 3402.65, 3446.76 and 3560.86 cm^{-1} , respectively, with corresponding intensity of 467.955, 372.491, 332.24, 10.0712 and 365.915 km/mol. The Raman activity of these modes, respectively, is 11.961, 2.587, 59.191, 63.917 and 103.755 Å/a.m.u.

Table S6. Relative shifts in the scaled [Ref.47] vibrational (IR) frequency (in cm^{-1}), along with the corresponding intensity (in km/mol) depicted in parenthesis, and Raman activity (in Å/a.m.u.), for relevant vibrational modes in various complexes of *L*-proline with single water molecule with respect to lowest-lying Complex 4b at DFT/BHandHLYP/6-311++G(d,p) level of the theory.

	L-Proline								water	
Modes	v (C=O)		v (C-O)		v(O-H)		v(N-H)		v_{sym}(O-H)	
Complexes	IR shift	Raman shift	IR shift	Raman shift	IR shift	Raman shift	IR shift	Raman shift	IR shift	Raman shift
Complex 3a	17.28		-85.26		272.44		17.34		14.53	
	(74.18)	-1.28	(59.94)	1.55	(-573.45)	-48.44	(30.81)	19.67	(45.73)	38.78
Complex 3b	-1.23		-100.54		-3.99		-7.08		4.85	
	(-15.84)	-1.46	(-134.35)	-0.51	(14.13)	-4.56	(6.83)	-13.84	(-16.56)	-0.21
Complex 3c	52.77		-117.87		271.42		-26.73		78.96	
	(29.75)	-0.13	(9.04)	0.09	(-515.85)	-26.21	(-0.52)	-14.89	(-183.90)	6.18
Complex 3d	37.60		-68.43		275.57		-32.06		-168.57	
	(10.09)	-2.33	(-1.640	0.43	(-558.85)	-51.08	(114.87)	16.36	(360.68)	75.67
Complex 3e	54.68		-82.60		276.82		-13.57		-88.66	
	(43.98)	-1.70	(11.20)	-0.22	(-558.08)	-55.61	(-12.85)	41.34	(255.62)	64.33
Complex 4a	19.74		-105.39		271.58		-12.95		26.60	
	(65.60)	-0.04	(-1.83)	-0.23	(-572.75)	-44.76	(78.78)	48.80	(-7.46)	37.29
Complex 4b*	0.00		0.00		0.00		0.00		0.00	
	(0.00)	0.00	(0.00)	0.00	(0.00)	0.00	(0.00)	0.00	(0.00)	0.00
Complex 4c	52.01		-113.93		269.40		4.02		75.79	
	(37.85)	0.90	(87.12)	-0.59	(-510.79)	-12.11	(-3.70)	0.95	(-170.90)	2.89
Complex 4d	39.66		-115.72		274.54		-26.57		-172.49	
	(28.93)	-0.82	(-42.91)	-0.45	(-559.26)	-45.96	(207.87)	48.31	(236.04)	43.86

* The IR frequency of vibrational modes, v(C=O), v (C-O), v(O-H), v(N-H) and v_{sym}(O-H, H_2O) in complex 4b is 1732.01, 1228.50, 3398.35, 3439.35 and 3601.15cm^{-1} , respectively, with corresponding intensity of 325.833, 205.575, 670.428, 23.104 and 261.831 km/mol. The Raman activity of these modes, respectively, is 11.276, 1.725, 70.181, 52.647 and 159.719 Å/a.m.u.

Table S7. Comparison of experimental frequencies and intensity from Ref. [51] with that of computed at BHandHLYP/6-311++G(d,p) with frequencies scaled with correction factor of 0.9335 [Ref. 47] for conformers P1 and P4. Values in parenthesis were computed at B3LYP/aug-cc-pVDZ level of the theory reported in previous work [Ref. 51].

Experimental		Computed						Experimental		Computed					
		P1			P4					P1			P4		
ν	I^a_{obs}	ν	I_{calc}		ν	I_{calc}		ν	I_{obs}	ν	I_{calc}		ν	I_{calc}	
3559	2.69				3674 (3588)	103.74 (65.9)	ν (OH)	1105	2.94	1102 (1105)	35.12 (30.5)	ν (N1C2)	1090 (1104)	8.31 (41.6)	ring bend
3545								1072	026	1061 (1076)	4.84 (8.7)	ring tor			
3393	0.54	3451 (3413)	10.14 (65.9)	ν (NH)				1021	0.12	1022 (1045)	2.89 (2.0)	ν (C2C4)	1029 (1049)	3.08 (1.9)	ν (C3C4)
3369	0.50				3440 (3396)	21.90 (16.3)	ν (NH)	976	0.04				963 (979)	7.31 (6.5)	ring bend
3025	5.20	3426 (3163)	318.67 (342.0)	ν (OH)				955	0.13	936 (952)	5.83 (5.7)	ring bend	941 (958)	2.25 (1.4)	ν (C3C4)
2984	2.10	2999 (3008)	8.77 (9.5)	ν (C4H)	2987 (2997)	29.66 (30.2)	ν (C4H)	950	0.23	933 (950)	4.41 (11.6)	ν (C2C4)			
		2980 (2990)	29.99 (27.3)	ν (CH)	2974 (2983)	29.40 (25.5)	ν (C1H)	916	0.16	887 (914)	37.74 (2.0)	ν (C3C4)			
2959	1.98	2956 (2961)	33.51 (34.7)	ν (CH)	2949 (2952)	51.72 (51.0)	ν (C3H)	907	0.17				891 (904)	1.34 (1.0)	ring bend
2934	2.34	2949 (2948)	24.71 (28.1)	ν (CH)	2926 (2935)	22.64 (17.7)	ν (C4H)	899	0.97	896 (922)	29.82 (76.2)	OH tor	903 (922)	0.26 (0.2)	ν (C1C3)
		2928 (2935)	22.42 (14.4)	ν (CH)				896							
2916		2921 (2930)	10.42 (13.3)	ν (CH)	2922 (2931)	14.14 (19.6)	ν (C3H)	884	0.65	861 (899)	22.97 (7.7)	ϖ (N1C2C5)			
2885	2.28				2902 (2892)	26.22 (26.6)	ν (C2H)	876	0.42	854 (871)	21.61 (4.4)	ring bend	860 (873)	10.41 (14.1)	ring bend
2865	1.19	2885 (2884)	57.38 (64.4)	ν (CH)				853	0.35						
2846					2851 (2847)	68.37 (74.9)	ν (C1H)	844	0.31	820 (847)	18.57 (7.0)	O2C5C2C4 tor	837 (849)	6.14 (7.8)	N1C2C5O1 tor
1795								822	0.06						
1789	7.22	1801 (1803)	413.12 (360.5)	ν (C=O)				782	0.46	782 (793)	9.29 (3.8)	ν (C2C5)			
1781								768	0.60				762 (772)	84.48 (67.2)	NH tor
1766	6.03				1774 (1774)	352.84 (286.1)	ν (C=O)	751	0.18						
1488	0.05	1480 (1499)	2.57 (3.2)	ϖ (CH)	1480 (1499)	1.99 (1.9)	ϖ (CH)	726	0.85	719 (724)	20.21 (15.1)	N1C2C5O1			
		1455 (1476)	7.08 (5.9)	ϖ (CH)	1454 (1476)	3.02 (2.4)	ϖ (CH)	713	0.58				706 (710)	46.95 (35.9)	N1C2C5O1 tor
1463	0.29	1445 (1464)	6.42 (5.2)	ϖ (CH)	1442 (1461)	5.68 (4.1)	ϖ (NH)	675	0.53						
1451	0.52				1433 (1446)	8.36 (10.3)	ϖ (CH)	668							
1412	2.28	1383 (1425)	364.4 (213.2)	ϖ (OH) and ν (C-O)				663							
1405	1.40							628	0.43				625 (632)	56.77 (61.6)	O1C5C2C4 tor
1384	6.23	1406 (1407)	71.56 (151.6)	ϖ (NH)				621	0.45	611 (623)	26.44 (20.5)	N1C2C5O2 tor			
1381								603	0.24				593 (605)	33.49 (20.7)	ϖ (C2C5O1)
1364	0.83				1358 (1364)	48.76 (29.9)	ϖ (CH)	597	0.21	572 (582)	8.55 (5.9)	ϖ (C2C5O1)			
1350	0.54	1343 (1349)	3.19 (6.5)	ϖ (CH)				584							
1330	0.10				1327 (1335)	31.43 (25.5)	ϖ (CH)	576	0.52				561 (579)	33.02 (19.3)	OH tor
1320	0.12	1312 (1324)	2.66 (2.1)	ϖ (CH)	1305 (1318)	3.88 (0.5)	ϖ (CH)	569	0.44						
1294		1287 (1298)	0.55 (12.6)	ϖ (CH)	1293 (1303)	1.62 (1.8)	ϖ (CH)	564		554 (570)	7.23 (6.9)	ring bend	0		
1286	0.32	1284 (1294)	33.33 (11.9)	ϖ (CH)	1270 (1285)	15.36 (5.7)	ϖ (OH)	560					0		
					1262 (1272)	1.89 (2.4)	ϖ (CH)	551	0.17				0		
1247	0.10	1236 (1249)	10.91 (8.1)	ϖ (CH)				546	1.26				536 (549)	53.08 (44.3)	OH tor
		1218	1.79		1216	0.48	ϖ	541							

		(1227)	(1.9)		(1230)	(0.4)	(N1C2C5)								
1210	0.25									459 (461)	3.03 (2.3)	ϖ (C2C5O2)	407 (411)	15.34 (15.1)	ϖ (C2C5O2)
1206		1197 (1205)	11.28 (17.5)	ν (C5O1)						329 (331)	8.22 (10.9)	N1C2C3 bend	284 (286)	10.16 (10.5)	ϖ (N1C2C5)
		1173 (1182)	3.54 (1.9)	ϖ (CH)	1180 (1187)	14.71 (8.5)	ϖ (CH)			288 (288)	6.88 (6.2)	ring tor	258 (259)	0.97 (0.9)	ring tor
1150					1162 (1166)	88.10 (60.0)	ν (N1C2)			198 (201)	6.40 (6.6)	ring tor	190 (194)	0.47 (0.5)	ring tor
					1147 (1160)	10.7 (6.3)	ϖ (CH)			105 (109)	0.69 (0.6)	ring tor	62 (60)	1.54 (1.5)	O1C5C2C4 tor
1142	2.21	1139 (1148)	22.86 (27.5)	ν (C5O1)						50 (55)	2.74	O2C5C2C4	43 (42)	1.34 (1.2)	ring tor
1109	2.77				1121 (1120)	235.0 (221.7)	ν (C5O2)								

${}^{a}I_{obs}$ is experimental relative integral intensities* ν= stretching, ϖ=bend , tor=torsion

Table S8. Relative shifts in the scaled [Ref.47] vibrational (IR) frequency (in cm^{-1}), along with the corresponding intensity (in km/mol) depicted in parenthesis, and Raman activity (in Å/a.m.u.), for relevant vibrational with respect to P1, at DFT/BHandHLYP/6-311++G(d,p) level of the theory.

Modes	*ν* (C=O)		*ν* (C-O)		*ν*(O-H)		*ν*(N-H)	
Species	IR shift	Raman shift	IR shift	Raman shift	IR shift	Raman shift	IR shift	Raman shift
P1	0.0		0.0		0.0		0.0	
	(0.0)	0.0	(0.0)	0.0	(0.0)	0.0	(0.0)	0.0
Complex 1a	-20.85		-35.46		28.89		-76.33	
	(-105.52)	-0.99	(-157.51)	1.39	(812.89)	-18.88	(35.56)	50.89
Complex 1b	-14.75		1.16		-36.51		-1.33	
	(32.08)	0.75	(-15.86)	-0.25	(56.36)	-1.04	(1.04)	5.37
Complex 1c	-28.40		9.34		-45.50		-4.96	
	(43.16)	0.39	(-77.48)	-0.76	(34.72)	-3.32	(0.46)	6.97
Complex 1d	5.38		-0.02		245.37		0.32	
	(0.02)	-0.83	(-5.11)	0.30	(-214.02)	25.84	(-0.03)	9.58
Complex 1e	-4.32		13.29		-59.95		-26.60	
	(18.07)	0.18	(32.99)	0.18	(63.69)	-0.24	(137.43)	37.00
P1 in water	-58.55		-7.36		-171.60		-8.41	
as solvent	(348.78)	13.69	(266.68)	4.48	(369.83)	65.63	(17.46)	95.45

Table S9. Relative shifts in the scaled [Ref.47] vibrational (IR) frequency (in cm^{-1}), along with the corresponding intensity (in km/mol) depicted in parenthesis, and Raman activity (in Å/a.m.u.), with respect to conformer P2, at DFT/BHandHLYP/6-311++G(d,p) level of the theory.

Modes	*ν* (C=O)		*ν* (C-O)		*ν*(O-H)		*ν*(N-H)	
Species	IR shift	Raman shift	IR shift	Raman shift	IR shift	Raman shift	IR shift	Raman shift
P2	0.0		0.0		0.0		0.0	
	(0.0)	0.0	(0.0)	0.0	(0.0)	0.0	(0.0)	0.0
Complex 2a	-22.04		-32.55		1.84		-51.87	
	(-21.53)	4.02	(-160.99)	-1.01	(775.88)	-56.59	(-122.35)	54.37
Complex 2b	-14.59		3.31		201.15		-3.84	
	(32.94)	0.88	(-15.36)	-0.30	(129.79)	47.35	(-120.81)	31.92
Complex 2c	-28.58		12.73		-41.18		-5.10	
	(41.18)	0.33	(-38.23)	-0.49	(157.26)	-30.21	(-121.18)	33.14
Complex 2d	4.98		4.40		-74.80		-10.15	
	(0.49)	-0.37	(-12.43)	0.29	(164.32)	-38.46	(-124.08)	40.36
Complex 2e	-4.29		13.39		-51.67		-26.90	
	(16.58)	0.05	(11.92)	0.49	(190.70)	-22.30	(7.27)	58.09
P2 in water	-59.29		-8.58		-158.21		-6.74	
as solvent	(341.33)	13.78	(250.38)	5.95	(466.84)	31.79	(-107.87)	107.77

Table S10. Relative shifts in the scaled [Ref.47] vibrational (IR) frequency (in cm^{-1}), along with the corresponding intensity (in km/mol) depicted in parenthesis, and Raman activity (in Å/a.m.u.), with respect to conformer P3, at DFT/BHandHLYP/6-311++G(d,p) level of the theory.

Modes	ν (C=O)		ν (C-O)		ν(O-H)		ν(N-H)	
Species	IR shift	Raman shift	IR shift	Raman shift	IR shift	Raman shift	IR shift	Raman shift
P3	0.0		0.0		0.0		0.0	
	(0.0)	0.0	(0.0)	0.0	(0.0)	0.0	(0.0)	0.0
Complex 3a	-22.33		24.05		-3.89		23.34	
	(63.64)	0.74	(59.77)	2.12	(-8.53)	3.17	(25.52)	33.48
Complex 3b	-40.84		8.77		-280.32		-1.07	
	(-26.37)	0.56	-134.52	0.06	579.05	47.05	(1.54)	-0.02
Complex 3c	13.16		-8.57		-4.92		-20.72	
	(19.22)	1.89	8.87	0.65	49.07	25.40	(-5.81)	-1.08
Complex 3d	-2.01		40.87		-0.77		-26.05	
	(-0.44)	-0.30	-1.81	1.00	6.07	0.53	(109.58)	30.18
Complex 3e	15.08		26.71		0.49		-7.57	
	(33.45)	0.32	11.02	0.34	6.84	-4.00	(-18.14)	55.16
P3 in water	-41.38		-17.69		-23.48		-34.75	
as solvent	(298.62)	13.51	6.11	4.41	66.41	43.75	(5.16)	58.13

Table S11. Relative shifts in the scaled [Ref.47] vibrational (IR) frequency (in cm^{-1}), along with the corresponding intensity (in km/mol) depicted in parenthesis, and Raman activity (in Å/a.m.u.), with respect to conformer P4, at DFT/BHandHLYP/6-311++G(d,p) level of the theory.

Modes	ν (C=O)		ν (C-O)		ν(O-H)		ν(N-H)	
Species	IR shift	Raman shift	IR shift	Raman shift	IR shift	Raman shift	IR shift	Raman shift
P4	0.0		0.0		0.0		0.0	
	(0.0)	0.0	(0.0)	0.0	(0.0)	0.0	(0.0)	0.0
Complex 4a	-21.71		2.19		-4.22		-13.09	
	(38.59)	0.62	(-31.27)	0.16	(-6.05)	-0.30	(79.99)	47.60
Complex 4b	-41.46		107.59		-275.80		-0.14	
	(-27.01)	0.66	(-29.43)	0.39	(566.69)	44.46	(1.21)	-1.20
Complex 4c	10.55		-6.35		-6.40		3.88	
	(10.84)	1.57	(57.68)	-0.20	(55.90)	32.36	(-2.49)	-0.26
Complex 4d	-1.80		-8.13		-1.26		-26.71	
	(1.92)	-0.16	(-72.34)	-0.05	(7.43)	-1.50	(209.07)	47.11
P4 in water	-44.01		-11.70		-23.11		-9.17	
as solvent	(294.02)	14.72	(97.08)	1.70	(62.70)	49.54	(7.49)	74.49

Table S12. Standard Gibbs free energy change (ΔG) in kcal/mol, at various temperatures, for the dissociation pathways at BHandHLYP/6-311++G(d,p) level of the theory depicted in supporting information Figure S1.

Dissociation	Temperature (K)		
pathways	200	298.15	400
P4→DC4	87.98	86.47	84.59
P4→DC5	91.74	90.05	88.04
P4→DC6	38.97	37.40	35.71
P4→DC7	29.56	27.80	25.79
P4→DC8	17.95	15.94	13.62
P4→DC9	13.05	9.29	5.02
P4→DC10	44.43	43.49	42.55
P3→DC2	49.82	48.26	46.44

Input and options applied in some calculations

1. Input file for GRRM search around proline conformer P4

```
# GRRM/HF/6-31G

0 1
N     -0.076405   0.150621   0.008484
C      0.006116  -0.006859   1.458318
C      1.233131   0.107601  -0.614375
H     -0.040922  -1.049141   1.772060
H     -0.797754   0.527159   1.945657
C      1.381901   0.586789   1.768590
C      2.237316   0.137677   0.572774
H      1.387454   0.964084  -1.260831
C      1.426627  -1.113731  -1.470721
H      1.785396   0.245175   2.712860
H      1.314804   1.667631   1.800120
H      2.638071  -0.853007   0.753986
H      3.072641   0.791896   0.372192
O      0.622618  -2.004112  -1.643720
H     -0.813363  -0.316211  -0.469753
O      2.635345  -1.118468  -2.076839
H      2.785571  -1.876860  -2.636542
options
FirstOnly
```

2. Input file for IRC around ComplexTS1a/Z1

```
#IRC/BHandHLYP/6-311++G**

0 1
N     -0.158877286333     -0.144650112479      0.305019366169
C      0.469552916715     -0.158344585178      1.661964468285
C      0.951603058832      0.001014566377     -0.686475444246
H      0.451524571280     -1.177237044750      2.024758919719
H     -0.130721859561      0.448574295763      2.327747168314
C      1.896261856260      0.380031994230      1.469509094772
C      1.916742693544      0.925011907136      0.040278320455
H      0.546232568915      0.435009734377     -1.593950352345
C      1.637592045152     -1.330173836156     -1.107771905497
H      2.613983359560     -0.426674617035      1.565637824155
H      2.145760036717      1.132734211577      2.207501640293
H      2.895539007249      0.897846855757     -0.414865014360
H      1.545652840706      1.947521386135      0.011070065695
H     -0.757001840042      0.662771685588      0.224291864765
O      1.009416342054     -2.429467499600     -0.954390009519
H     -0.098274028096     -2.473383647541     -0.564530523541
O      2.734526159566     -1.203764682405     -1.590309586222
O     -1.185532324675     -2.332872099609     -0.074746058574
H     -0.803830683178     -1.097493264619      0.125131295781
H     -1.904359122662     -2.561003376557     -0.651429645098
options
DownDC=15
```

3. Input file for IRC around ComplexTS1a/2a

```
#IRC/BHandHLYP/6-311++G**

0 1
N    -0.040071056520   -0.165154322079    0.177304930972
C     0.313447665091   -0.203476893483    1.602435189345
C     1.240921336658   -0.093227746442   -0.540882166436
H     0.603021405737   -1.220187393780    1.855440759516
H    -0.544092516904    0.055998845018    2.212333194238
C     1.494653256803    0.750396409830    1.741466131193
C     2.264306935639    0.558323589972    0.427774751255
H     1.107712701438    0.510091128456   -1.433634478667
C     1.773710619903   -1.426521868951   -1.074337588845
H     2.102901559360    0.542171912465    2.614516522049
H     1.130837120611    1.770975396898    1.831605204823
H     3.119767706015   -0.092516653842    0.549206497685
H     2.635891449269    1.495816150316    0.033015665164
H    -0.532946585208    0.695598129857    0.001791046691
O     0.963215485097   -2.459612765878   -1.181730292165
H     0.056524479177   -2.326108793744   -0.876936445258
O     2.910790473278   -1.498658659336   -1.427323532831
O    -1.688112720650   -2.362217058438   -0.353810332977
H    -1.450633163633   -1.452502352331   -0.139954303340
H    -2.443613378157   -2.347279279485   -0.929971518403
options
DownDC=15
```

4. Input file for IRC around ComplexTS1a/1b

```
# IRC/BHandHLYP/6-311++G**

0 1
N     0.477457099270    0.926787305315    0.424400734740
C     0.373145316872    0.374044958682    1.783820236039
C     1.796112269029    0.601141029312   -0.131418445542
H    -0.617310875809   -0.033973261636    1.964126792623
H     0.557469570544    1.139106602840    2.537818283966
C     1.460371233040   -0.690162971776    1.841742343939
C     2.572681199084   -0.072425383498    1.002617796488
H     2.304635100902    1.498020007855   -0.476017341474
C     1.719887176883   -0.298158818979   -1.367855751607
H     1.110715153753   -1.611199750450    1.381956166692
H     1.761978122467   -0.919039574699    2.857293306916
H     3.295257240323   -0.783285514602    0.626563700347
H     3.101448934617    0.680258854014    1.581211877650
H     0.307517078583    1.914476329051    0.410166425582
O     0.558611614589   -0.369966911784   -1.986671272982
H    -0.133877733654    0.129692403240   -1.535320356919
O     2.683775684245   -0.874903050515   -1.770911164489
O    -1.944009786946    0.791288709105   -1.375111289447
H    -1.999902714954    0.703908452835   -0.429275810661
H    -2.705930513214    0.355134591008   -1.741542351016
options
```

DownDC=15